Characterization of Homonuclear Spin Pairs from Two-Dimensional Spin–Echo NMR Powder Patterns

Toshihito Nakai and Charles A. McDowell*

Contribution from the Department of Chemistry, University of British Columbia, 2036 Main Mall, Vancouver, British Columbia, Canada V6T 1Z1

Received January 14, 1994®

Abstract: Measurements of two-dimensional (2D) solid-state NMR spectra of homonuclear spin-$^1/_2$ pairs in stationary polycrystalline samples, reflecting dipolar and J couplings as well as anisotropic chemical shift interactions, are described. To obtain the correlation of the powder patterns in the 2D frequency plane, a π-pulse spin–echo subsequence is incorporated into the evolution period of the 2D pulse sequence. In general, the spin-echo sequence does not perfectly refocus the influences of the chemical shift interactions, but such residual chemical shifts may cause complicated powder patterns in the relevant frequency dimension instead of the well-known Pake patterns. The analysis of the 2D spin-echo powder patterns thus obtained for ^{31}P–^{31}P systems in tetraphenyldiphosphine and sodium pyrophosphate decahydrate and a ^{13}C–^{13}C system in 1,2-^{13}C doubly-labeled palmitic acid has yielded their spin parameters; in spectral simulations, the residual chemical shift effects play an important role in giving correct and, in some cases, otherwise unobtainable parameters. Information on molecular structures, such as internuclear directions with respect to the principal axis systems of the chemical shift tensors, has been obtained for the above compounds. In particular, the conformation of the molecules in the crystalline systems has been clarified and discussed in detail.

Introduction

In solid-state nuclear magnetic resonance (NMR) spectroscopy, dipolar coupled spin systems have often been studied to obtain information on molecular structures and dynamics.[1] If the coupled two spins of interest are spatially well separated from other spins, their NMR spectra may clearly and directly yield the distances and the directions of these particular spins; for powdered or polycrystalline samples, which are much more widely available than single crystals, the spectra manifest characteristic distributions of resonance lines known as Pake patterns,[2] reflecting the internuclear distances. Furthermore, if other anisotropic spin interactions such as chemical shifts are observed in addition to the couplings, the spectra even for polycrystalline samples may reflect the relative orientations of the interaction tensors with respect to the dipolar axis or internuclear directions without appealing to single-crystal measurements; the orientations of the involved interaction tensors are internally fixed in molecules and not averaged out by integrating over all crystallite orientations. Therefore, the analysis of the powder patterns for coupling spin systems is important, and in fact several authors have described the details.[3-5]

The measurements of two-dimensional (2D) powder patterns were proposed as a means to determine the above spin parameters with high accuracy.[4a] In the present study, we consider 2D powder patterns reflecting different interactions in the two distinct frequency dimensions.[4,5] To obtain such 2D powder patterns for homonuclear spin systems,[5] a π-pulse spin-echo sequence[6] has simply been employed in the evolution (t_1) period to modify the effective Hamiltonian, whereas in the detection (t_2) period, the inherent Hamiltonian dominates the spin systems; the applied spin-echo sequence has been expected to cancel chemical shift evolution.[4c-f,5] We refer to the resultant spectra observed for stationary polycrystalline samples as 2D spin-echo powder patterns, which we treat in this study. Here may arise an interesting point: in spite of its original purpose, the spin-echo sequence may generally not refocus and remove the chemical shift interactions completely if applied to homonuclear spin systems. In fact, 2D J spectroscopy for solutions,[7] where the echo sequence is incorporated, yields rather complicated spectra for the homonuclear system having a strong coupling compared with a chemical shift difference of involved two spins[7b,c] because of the imperfect refocusing of the chemical shifts. A similar theoretical treatment for the strong coupling effects should generally be necessary to analyze the 2D spin-echo powder patterns of homonuclear coupled spin systems in solids. However, such careful analysis has not been reported, and on the contrary the complete refocusing of the chemical shifts has tacitly been assumed to be the effect of the spin-echo sequence.[5]

In the present sudy, we describe the precise effects of the spin-echo sequence on homonuclear spin pair systems. Thereby, we establish the correct analysis for the 2D spin-echo powder patterns and demonstrate the strong coupling or residual chemical shift effects in solids by spectral simulations. As applications, attempts are made to determine the spin parameters and thus to characterize spin systems through the 2D powder patterns observed for some ^{31}P–^{31}P and ^{13}C–^{13}C homonuclear spin systems.

Experimental Section

As homonuclear coupled two-spin systems we chose two ^{31}P compounds, tetraphenyldiphosphine, $(C_6H_5)_2PP(C_6H_5)_2$, and sodium pyrophosphate

* Abstract published in *Advance ACS Abstracts*. June 15, 1994.

(1) Abragam, A. *Principles of Nuclear Magnetism*; Oxford University: Oxford, U.K., 1961.

(2) Pake, G. E. *J. Chem. Phys.* **1948**, *16*, 327–336.

(3) (a) VanderHart, D. L.; Gutowski, H. S. *J. Chem. Phys.* **1968**, *49*, 261–271. (b) Zilm, K. W.; Grant, D. M. *J. Am. Chem. Soc.* **1981**, *103*, 2913–2922. (c) Power, W. P.; Wasylishen, R. E. *Annu. Rep. NMR Spectrosc.* **1991**, *23*, 1–84.

(4) (a) Linder, M.; Höhener, A.; Ernst, R. R. *J. Chem. Phys.* **1980**, *73*, 4959–4970. (b) Maas, W. E. J. R.; Kentgens, A. P. M.; Veeman, W. S. *J. Chem. Phys.* **1987**, *87*, 6854–6858. (c) Nakai, T.; Terao, T.; Shirakawa, H. *Chem. Phys. Lett.* **1988**, *145*, 90–94. (d) Nakai, T.; Ashida, J.; Terao, T. *J. Chem. Phys.* **1988**, *88*, 6049–6058; (e) *Mol. Phys.* **1989**, *67*, 839–847; (f) *Magn. Reson. Chem.* **1989**, *27*, 666–668.

(5) (a) Duijvestijn, M. J.; Manenschijn, A.; Smidt, J.; Wind, R. A. *J. Magn. Reson.* **1985**, *64*, 461–469. (b) Zilm, K. W.; Webb, G. G.; Cowley, A. H.; Pakulski, M.; Orendt, A. *J. Am. Chem. Soc.* **1988**, *110*, 2032–2038. (c) Weliky, D. P.; Dabbagh, G.; Tycko, R. *J. Magn. Reson.* **1993**, *A104*, 10–16.

(6) Hahn, E. L. *Phys. Rev.* **1950**, *80*, 580–594.

(7) (a) Aue, W. P.; Karhan, J.; Ernst, R. R. *J. Chem. Phys.* **1976**, *64*, 4226–4227. (b) Kumar, A. *J. Magn. Reson.* **1978**, *30*, 227–249. (c) Bodenhausen, G.; Freeman, R.; Morris, G. A.; Turner, D. L. *J. Magn. Reson.* **1978**, *31*, 75–95.

0002-7863/94/1516-6373$04.50/0

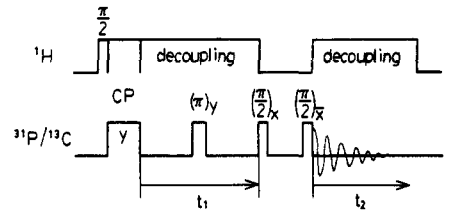

Figure 1. Pulse sequence for measuring the homonuclear 2D spin–echo powder patterns.

decahydrate, $Na_4P_2O_7{\cdot}10H_2O$, and a ^{13}C doubly-labeled compound of 1,2-^{13}C palmitic acid, $CH_3(CH_2)_{13}{}^{13}CH_2{}^{13}COOH$; the samples of the phosphorus compounds were purchased from Aldrich Chemical Co., while the 99% ^{13}C pairwise-enriched sample was purchased from Cambridge Isotope Laboratory.

The NMR experiments were performed on a Bruker MSL200 spectrometer with operating resonance frequencies of 81.015 MHz for ^{31}P, 50.330 MHz for ^{13}C, and 200.13 MHz for ^1H. A solid-state magic-angle spinning (MAS) probe from Doty Scientific, Inc. was employed even for the experiments with static samples.

The radio frequency (rf) pulse sequence for the measurements of the 2D spin-echo powder patterns is shown in Figure 1. The pulse sequence involves a π-pulse spin-echo subsequence in the t_1 period, similar to that used for homonuclear 2D J spectroscopy for solutions.[7] The obtained 2D free induction decays (FIDs) $s(t_1,t_2)$ yield the 2D powder patterns $S(F_1,F_2)$ after the Fourier transformation with respect to both t_1 and t_2. The summations of the resultant 2D spectra onto the F_1 and the F_2 axes, respectively, correspond to 1D spin-echo powder patterns and conventional 1D dipolar (and J)/chemical shift powder patterns. An important feature of the pulse sequence is the incorporation of a z-filter period[8] between the t_1 and the t_2 periods; only the y component of the t_1-evolved magnetizations is stored along the z (external field) direction and reconverted to observables in the t_2 period. Thereby, pure absorptive 2D line shapes can be obtained from the resultant amplitude-modulated FIDs by employing the time-proportional phase-increment (TPPI)[9] Fourier transformation. The achieved higher resolution than that of magnitude-mode spectra[5a] may reveal the details of the ridges in the 2D powder patterns. The 2D spectra resulting from the above procedure are symmetrized with respect to $F_1 = 0$. As we will show below, this data processing, however, does not degrade the information reflected in the spin-echo powder patterns along the F_1 axis, which are inherently symmetric.

Theoretical 2D spectra were calculated on an IBM-RISC 6000 computer, connected with an NCD15r x-terminal, from a program written in FORTRAN-77. The program gives resonance signals on the 2D plane for many crystallite orientations, executes convolution for them, and draws the contour plotting of the 2D spectra, with the CPU time less than 1 s if we consider a small number (e.g., 10 000) of orientations for rough estimation of the spin parameters. To refine the initial parameters obtained in this way, typically 360 × 360 different orientations were involved in the calculations, which then took a CPU time of about 4 s.

Theory

The 2D FID obtained with the pulse scheme shown in Figure 1 is an amplitude-modulated one, and its expresion can be factorized as $s(t_1,t_2) = s(t_1)s(t_2)$. Namely, we can separately consider the t_1 FID $s(t_1)$ and the t_2 FID $s(t_2)$. With a careful treatment described below, we will obtain an exact expression for $s(t_1)$ reflecting the effect of the spin-echo sequence and examine how the residual chemical shifts affect the spectra in the F_1 dimension. On the other hand, we will briefly discuss $s(t_2)$ arising from the ordinary free precession of magnetizations, which has already been studied in detail.[3b] We will then demonstrate the 2D powder patterns constructed from the FIDs $s(t_1)$ and $s(t_2)$.

We consider the following secular Hamiltonian for homonuclear coupled spins I_1 and I_2, involving the anisotropic J coupling:[3b,5b,10]

$$\begin{aligned}\mathcal{H} &= \Omega_1 I_{1z} + \Omega_2 I_{2z} + {}^1/_2 D_{zz}(3I_{1z}I_{2z} - \mathbf{I}_1\cdot\mathbf{I}_2) + \\ &\quad J_{zz}I_{1z}I_{2z} + {}^1/_4(J_{xx}+J_{yy})(I_{1+}I_{2-} + I_{1-}I_{2+}) \\ &= {}^1/_2\Sigma(I_{1z}+I_{2z}) + {}^1/_2\Delta(I_{1z}-I_{2z}) + \\ &\quad 2AI_{1z}I_{2z} + {}^1/_2B(I_{1+}I_{2-} + I_{1-}I_{2+}) \quad (1)\end{aligned}$$

with

$$\Sigma = \Omega_1 + \Omega_2, \quad \Delta = \Omega_1 - \Omega_2$$

$$A = {}^1/_2(D_{zz} + J_{zz}), \quad B = {}^1/_2(-D_{zz} + 3J_{iso} - J_{zz}) \quad (2)$$

where Ω_1 and Ω_2 are the chemical shift (offset) frequencies and D_{ii} and J_{ii} respectively signify the dipolar and the J coupling tensor components in the laboratory frame, whereas the isotropic J coupling ${}^1/_3(J_{xx} + J_{yy} + J_{zz})$ is denoted as J_{iso}. The above notation is convenient in that it can describe, by altering the definitions of the terms A and B, the cases without the J anisotropy ($A = {}^1/_2(D_{zz} + J_{iso})$, $B = -{}^1/_2D_{zz} + J_{iso}$) and furthermore the cases without the J coupling itself ($A = -B = {}^1/_2D_{zz}$). The frequencies Ω_1, Ω_2, D_{zz}, and J_{zz} (or Σ, Δ, A, and B) are expressed with the principal components of the corresponding interaction tensors and the Euler angles specifying the tensor principal axis orientations with respect to the laboratory frame in a well-established manner.[11]

Note that the Hamiltonian in eq 1 involves a flip-flop spin part $I_{1+}I_{2-} + I_{1-}I_{2+}$, which is not negligible except in the weak coupling limit, i.e., $|\Delta| \gg |B|$. This condition may not be satisfied even if the isotropic chemical shifts of the two spins are far apart, since the quantities Δ and B vary their magnitudes depending on the tensor axis or crystallite orientations in polycrystalline samples. Therefore, various strong coupling effects caused by the flip-flop term, which are known in solution-state NMR,[12] are generally to be expected for homonuclear coupled spin systems in solids.

The effect of the spin-echo sequence, $t_1/2$–$(\pi)_y$–$t_1/2$, can be evaluated in a compact form by using the product operator formalism[13] which we recently developed to apply to strongly coupled spins;[14] the density matrix calculations may yield the equivalent results but would be tedious. According to the reported result, the relevant part of the evolution is represented as[14a]

$$\begin{aligned}I_y \xrightarrow{t_1/2-(\pi)_y-t_1/2} I_y[&(\cos^2 2\theta + \sin^2 2\theta \cos {}^1/_2Rt_1)\cos At_1 + \\ &\sin 2\theta \sin {}^1/_2Rt_1 \sin At_1] \quad (3)\end{aligned}$$

where the quantities

$$R = (\Delta^2 + B^2)^{1/2}$$

$$\cos 2\theta = \Delta/R, \quad \sin 2\theta = B/R \quad (4)$$

are the well-known parameters describing the eigenvalues and the eigenstates of two-spin systems.[1,15] In eq 3, we have omitted the other possible spin operators fanned out from the initial state

(8) Sørensen, O. W.; Rance, M.; Ernst, R. R. *J. Magn. Reson.* **1984**, *56*, 527–534.
(9) (a) Marion, D.; Wüthrich, K. *Biochem. Biophys. Res. Commun.* **1983**, *113*, 967–974. (b) Nakai, T.; McDowell, C. A. *J. Magn. Reson.* **1993**, *A104*, 146–153.
(10) (a) Tutunjian, P. N.; Waugh, J. S. *J. Chem. Phys.* **1982**, *76*, 1223–1226; (b) *J. Magn. Reson.* **1982**, *49*, 155–158. (c) Pyykkö, P.; Wiesenfeld, L. *Mol. Phys.* **1981**, *43*, 557–580. (d) Jameson, C. J. In *Multinuclear NMR*; Mason, J., Ed.; Plenum: New York, 1987. (e) Lounila, J.; Kokisaari, J. *Prog. Nucl. Magn. Reson. Spectrosc.* **1982**, *15*, 249–290. (f) Challoner, R.; Nakai, T.; McDowell, C. A. *J. Magn. Reson.* **1991**, *94*, 433–438.
(11) Mehring, M. *High Resolution NMR in Solids*, 2nd ed.; Springer-Verlag: Berlin, 1983.
(12) Ernst, R. R.; Bodenhausen, G.; Wokaun, A. *Principles of Nuclear Magnetic Resonance in One and Two Dimensions*; Oxford University: Oxford, U.K., 1986.
(13) Sørensen, O. W.; Eich, G. W.; Levitt, M. H.; Bodenhausen, G.; Ernst, R. R. *Prog. Nucl. Magn. Reson. Spectrosc.* **1983**, *16*, 163–192.
(14) (a) Nakai, T.; McDowell, C. A. *Mol. Phys.* **1993**, *79*, 965–983; (b) *Mol. Phys.* **1994**, *81*, 337–358.
(15) Pople, J. A.; Schneider, W. G.; Bernstein, H. J. *High-resolution Nuclear Magnetic Resonance Spectroscopy*; McGraw-Hill: New York, 1959.

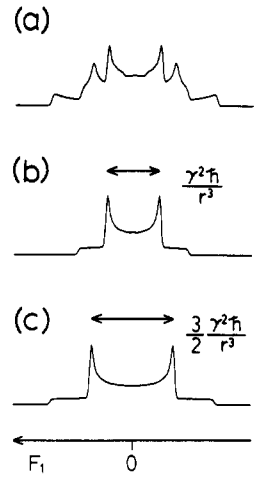

Figure 2. Simulated 1D spin-echo powder patterns for homonuclear spin pairs, or the F_1 projections of the 2D spin-echo powder patterns, arising from the t_1 FID $s(t_1)$. The spectra are calculated on the basis of eq 5 (a) without approximations, (b) in the AX approximation with $\sin 2\theta = 0$, and (c) in the A_2 approximation with $\cos 2\theta = 0$. The J couplings are disregarded.

I_y, such as $2I_{1z}I_{2x} + 2I_{1x}I_{2z}$, which are filtered out before the detection period.

From the coefficient of the evolved state given in eq 3, the expression for the t_1 FID $s(t_1)$ can straightforwardly be derived as

$$s(t_1) = \cos^2 2\theta[\exp(iAt_1) + \exp(-iAt_1)] + {}^1/_2 \sin 2\theta(1 + \sin 2\theta) \times [\exp\{i({}^1/_2R - A)t_1\} + \exp\{-i({}^1/_2R - A)t_1\}] - {}^1/_2 \sin 2\theta(1 - \sin 2\theta) \times [\exp\{i({}^1/_2R + A)t_1\} + \exp\{-i({}^1/_2R + A)t_1\}] \quad (5)$$

It follows that the resultant spectrum consists of six resonance lines along the F_1 axis for each crystallite orientation, similar to 2D J spectra for solutions.[7b,c] It should be noted that the lines at $F_1 = \pm({}^1/_2R \pm A)$ reflect the residual chemical shifts through the term R. By integrating the single-crystallite spectrum over all the orientations, we may obtain a 1D spin-echo powder pattern (Figure 2a) which is more complicated than well-known Pake patterns.[2]

It may be useful to clarify the relation between the above exact treatment and the following two types of approximations which have been used to describe the spin-echo powder patterns,[5] namely, the weak coupling (AX) approximation valid for the condition $|\Delta| \gg |B|$ and the magnetic equivalence (A_2) approximation for $|\Delta| \ll |B|$. For the former condition, simply by setting $\sin 2\theta = 0$ in the exact expression, we may obtain a doublet at $F_1 = \pm A$ for each crystallite. On the other hand, for the latter condition, depending on whether B is positive ($\sin 2\theta = +1$) or negative ($\sin 2\theta = -1$), either the doublet at $F_1 = \pm{}^1/_2(R - A)$ or the doublet at $F_1 = \pm{}^1/_2(R + A)$ becomes effective, and thus the spectrum always exhibits a single doublet at $F_1 = \pm({}^1/_2B - A)$. If we tentatively neglect the J contribution, the positions of the doublet peaks are $F_1 = \pm{}^1/_2D_{zz}$ in the AX approximation and $F_1 = \pm{}^3/_4D_{zz}$ in the A_2 approximation. For both cases, the corresponding powder patterns reflect only the dipolar coupling as Pake patterns,[2] the separations of the sharp singularities of which are given by $\gamma^2\hbar/r^3$ and ${}^3/_2\gamma^2\hbar/r^3$, respectively, as shown in Figures 2b and c. In turn, the spectrum reflecting the residual chemical shifts calculated without the above approximations (Figure 2a) is caused by the strong coupling or AB effect.

To examine the limitation of the AX and the A_2 approximations, we simulate in Figure 3a a series of 1D spin-echo powder patterns

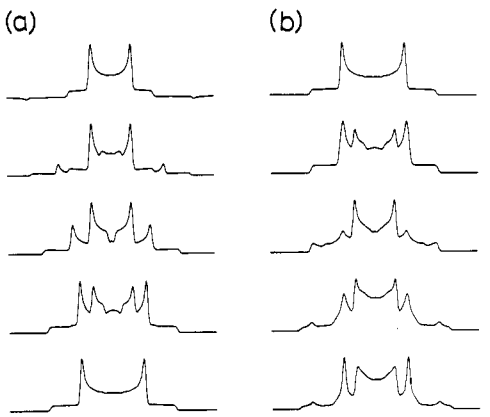

Figure 3. Simulated 1D spin-echo powder patterns for homonuclear spin pairs. (a) The difference of the isotropic chemical shifts for the two spins is varied as 10 (top), 3, 1.5, 0.7, and 0 kHz (bottom); the anisotropy of 5.25 kHz of axially symmetric shift tensors, which is common to both the spins, and the dipolar coupling constant $D = -2\gamma^2\hbar/r^3$ of −4.08 kHz are fixed. The spectral range is ±5 kHz. It is assumed that the two chemical shift tensors are collinear and their unique axes make an angle of 45° with the dipolar axis. (b) The mutual orientations of the two chemical shift tensors having the identical components are altered, whereas the other spin parameters are fixed and the same as those for (a); from the top to the bottom, the torsion angle between the two unique chemical shift axes around the dipolar axis is varied as 0, 20, 60, 150, and 180°.

ranging from the weak coupling limit (top) to the magnetic equivalence limit (bottom) without using these approximations. Only both the limits can be elucidated by the approximations, but in general the spectra exhibit various line shapes differing from Pake patterns. Also, in Figure 3b are shown another series of calculated spectra, for which we have assumed identical chemical shift components but varied the mutual orientations of the chemical shift axes for the two spins. As far as the shift tensor axes of the two spins do not coincide with each other, the striking AB effect exhibits itself in the spectra; in solids, only the cases of the identical shift components and the collinear shift axes can be described as A_2 spin systems because $\Delta = 0$ for all crystallite orientations. From the spectral simulations, we can at least conclude that clear and strict criteria for validating the AX and the A_2 approximations are not evident, since the critical frequencies in the laboratory frame Δ and B depend on various spin parameters which are usually unknown before simulating the experimental results. Therefore, it is obvious that the present exact treatment is necessary to analyze the spin-echo spectra accurately.

The evolution during the detection period t_2 can also be evaluated using the extended product operator theory as[14a]

$$I_y \xrightarrow{\mathcal{H}t_2} (I_y \cos {}^1/_2\Sigma t_2 - I_x \sin {}^1/_2\Sigma t_2) \times ({}^1/_2Rt_2 \cos At_2 + \sin 2\theta \sin {}^1/_2Rt_2 \sin At_2) \quad (6)$$

Thereby, the t_2 FID $s(t_2)$ is given by

$$s(t_2) = (1 - \sin 2\theta)\exp\{i[{}^1/_2(\Sigma + R) + A]t_2\} + (1 + \sin 2\theta)\exp\{i[{}^1/_2(\Sigma + R) - A]t_2\} + (1 + \sin 2\theta)\exp\{i[{}^1/_2(\Sigma - R) + A]t_2\} + (1 - \sin 2\theta)\exp\{i[{}^1/_2(\Sigma - R) - A]t_2\} \quad (7)$$

As in the classical analysis,[1,3b,15] the above formula leads to quartet lines for each crystallite. The powder average of the spectrum obviously causes both the dipolar and the chemical shift frequency distributions in the F_2 dimension.[3-5]

The 2D spin-echo spectrum is constructed simply by giving cross peaks on the (F_1,F_2) plane, the frequencies and the intensities of which are predicted from the forms of $s(t_1)$ and $s(t_2)$; because of the form of $s(t_1,t_2) = s(t_1)s(t_2)$, the peak at $(F_1,F_2) = (A, {}^1/_2(\Sigma$

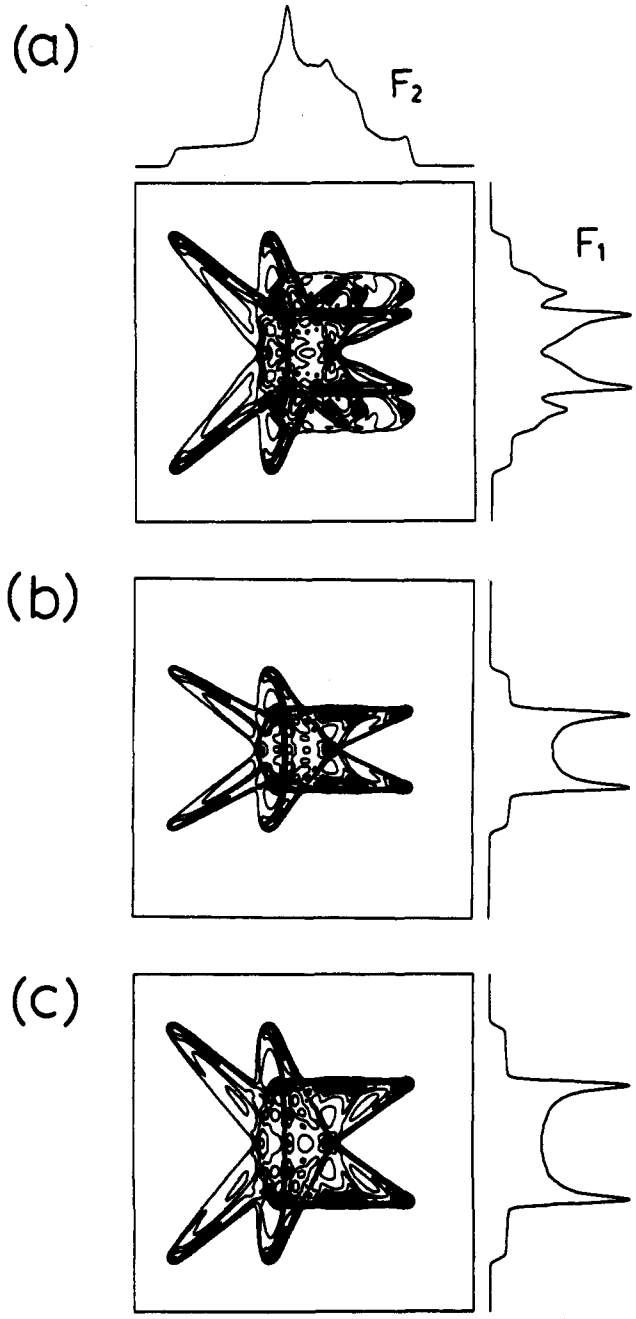

Figure 4. Simulated 2D spin-echo powder patterns for homonuclear spin pairs. The individual spectra are calculated (a) without approximations, (b) in the AX approximation, and (c) in the A_2 approximation.

$+ R) + A$), for example, possesses a relative intensity of $\cos^2 2\theta \times (1 - \sin 2\theta)$. Figure 4a illustrates an example of the calculated 2D powder pattern, obtained by integrating the 24 cross peaks over all possible crystallite orientations. As the AX and the A_2 approximations for the 2D powder patterns, we refer to the treatments to construct the spectra assuming the doublets at $F_1 = \pm A \simeq \pm {}^1/_2 D_{zz}$ and $\pm({}^1/_2 B - A) \simeq \mp {}^3/_4 D_{zz}$, respectively, predicted by the individual approximations; in the F_2 dimension, we assume the four peaks at $F_2 = {}^1/_2(\Sigma \pm R) \pm A$ even in these approximated treatments, following earlier studies.[5] The 2D powder patterns calculated in the AX and the A_2 approximations are shown in Figures 4b and c, respectively. Of course, these approximations generally manifest the 2D ridges different from those obtained in the exact calculation, and the spectral analysis based on them may lead to inaccurate spin parameters, even though earlier studies have employed these approximations.[5]

Clearly from the above discussion, the 2D spin-echo method generally does not separate the dipolar and the J couplings from the anisotropic chemical shifts in the F_1 dimension if applied to homonuclear spin systems. Nevertheless, the method is useful for determining the spin parameters with high accuracy, because the resultant 2D powder pattern may give rise to distinctive correlations between the effective Hamiltonians distinguished for the t_1 and the t_2 periods, as demonstrated in Figure 4. Since the 2D spin-echo powder pattern consists of the well-defined resonance frequencies and intensities as we have clarified above, the comparison between the experimental spectra and those calculated on the basis of the present theory is expected to lead to the correct evaluation of the spin parameters.

It is to be noted that the absolute signs of the terms A and B cannot be determined unambiguously, since the forms of the t_1 and the t_2 FIDs are invariant with the simultaneous exchange of the signs of these terms. We can know the parameters to which this ambiguity may have influences by making a usual assumption[3b,5b,10f] that the J tensor is axially symmetric and parallel to the dipolar tensor so that these terms are reduced to

$$A = {}^1/_2 D_{\text{eff}} f(\Omega) + {}^1/_2 J_{\text{iso}}, \quad B = -{}^1/_2 D_{\text{eff}} f(\Omega) + J_{\text{iso}} \quad (8)$$

The orientation dependence common to the dipolar and the J tensors is formally represented by $f(\Omega)$, and the effective coupling constant D_{eff} is given by

$$D_{\text{eff}} = -\frac{2\gamma^2\hbar}{r^3} + {}^2/_3(J_\parallel - J_\perp) \equiv D + \Delta J \quad (9)$$

where D is the pure dipolar coupling constant defined to be negative, while ΔJ is the anisotropy of the J coupling. Thus, from the terms A and B determined in the analysis of the 2D powder patterns, we may obtain the magnitudes and the relative signs of D_{eff} and J_{iso}. As reported earlier for ^{13}C–^1H and ^{13}C–^{13}C systems,[16] if the anisotropy of the J coupling ΔJ is negligible, the absolute sign of J_{iso} can be determined, since the sign of $D_{\text{eff}} = D$ is predetermined. In contrast, the presence of the J anisotropy may allow the positive and the negative effective coupling constants D_{eff}, in principle, the sign of J_{iso} being ambiguous. Furthermore, if we estimate the J anisotropy from the given magnitude $|D_{\text{eff}}|$ and the assumed value of D, there are two possibilities about its value[5b,10a,b] corresponding to the positive and the negative effective coupling constants, namely, $\Delta J = -D \pm |D_{\text{eff}}|$. However, one of these possibilities is often found preferable by intuition or theory, and the above ambiguity may be avoided.

It should be noted that the isotropic J coupling between homonuclear spins can be reflected in the spin-echo spectra. As is well known, this spin parameter is hidden for magnetically equivalent (A_2) spin systems[1,15] and cannot be obtained in the A_2 approximation, where the characteristic frequencies $\pm({}^1/_2 B - A) = \mp {}^3/_4 D_{\text{eff}} f(\Omega)$ exclude the term J_{iso}. Thus, in this sense, consideration of the residual chemical shifts in the exact calculations is important to estimate the value of J_{iso}; from the simulated F_1 projections for a spin pair having identical chemical shift components illustrated in Figure 5, we can recognize not only the presence of J_{iso} but also its sign relative to that of D_{eff}. A similar phenomenon of the appearance of J_{iso} for such spin pairs can take place in MAS spectra, which we have called J-recoupled spectra.[17]

The analysis of the 2D powder patterns to determine all spin parameters does not require any assumptions, except for the cases involving J anisotropy and then only to separate the information

(16) (a) Miura, H.; Terao, T.; Saika, A. *J. Chem. Phys.* **1986**, *85*, 2458–2462. (b) Terao, T.; Miura, H.; Saika, A. *J. Chem. Phys.* **1986**, *85*, 3816–3826. (c) Nakai, T.; McDowell, C. A. *Mol. Phys.* **1992**, *77*, 569–584; (d) *Bull. Magn. Reson.* **1993**, *15*, 149–153.

(17) (a) Nakai, T.; Challoner, R.; McDowell, C. A. *Chem. Phys. Lett.* **1991**, *180*, 13–18. (b) Challoner, R.; Nakai, T.; McDowell, C. A. *J. Chem. Phys.* **1991**, *94*, 7038–7045.

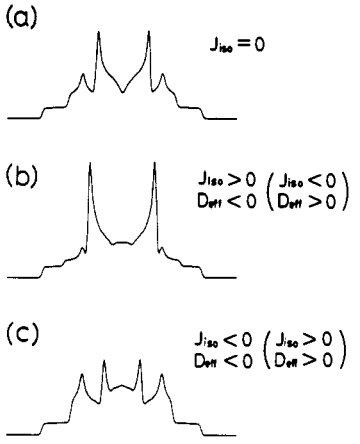

Figure 5. Simulated F_1 projections of the 2D spin-echo powder patterns for homonuclear spin pairs having identical chemical shift components, exhibiting the effects due to the isotropic J coupling. In contrast to (a) $J_{iso}=0$, the nonzero J_{iso} values having (b) the positive and (c) the negative signs are assumed, while the sign of the effective coupling constant D_{eff} is fixed to be negative. If D_{eff} is assumed to be positive, the spectra shown in (b) and (c) also correspond to the cases of the negative and the positive J_{iso} values, respectively.

on the J anisotropy ΔJ and the internuclear distance r from the effective coupling D_{eff}, so we may need previous knowledge of either $r(D)$ or ΔJ. Of course, further knowledge about the geometry of molecules may be helpful to reduce the number of the spin parameters. For example, the C_2 symmetry of molecules leads to identical chemical shift components for both the spins. As is usually the case with the spectra of coupled spin systems, the information obtained from spectral simulations is not only on the principal components of the individual interaction tensors but also on the relative orientations of the tensor principal axes.[3-5] There indeed exists an ambiguity if we attempt to specify the tensor orientations in the molecular frame but not in the other tensor axis frame because of the freedom of the overall rotation around the internuclear direction. In many cases, however, ambiguity may be avoided by assuming a typical or a reasonably acceptable direction for one of the chemical shift axes in the molecular frame.

Results and Discussion

Tetraphenyldiphosphine. The compound tetraphenyldiphosphine may be a good example to demonstrate the residual chemical shift effects in the 2D spin-echo powder pattern, as our preliminary report showed;[18] we here reinvestigate the spectra by considering the J coupling between the ^{31}P nuclei, unlike in the previous report.[18] More accurate spin parameters thus obtained are interpreted in terms of the molecular structure; neither X-ray studies nor single-crystal NMR studies have been reported on this compound. To our knowledge, the solid-state powder patterns for diphosphines R_2PPR_2 have not been analyzed in detail, and so the present study on tetraphenyldiphosphine may yield the first insights on anisotropic spin interactions in diphosphine molecules in the solid state.

Figure 6a illustrates the ^{31}P 2D spin-echo powder pattern observed for tetraphenyldiphosphine. It is of particular interest that the F_1 projection of the spectrum manifests an extra doublet at $F_1 = \pm 670$ Hz in addition to a Pake pattern; the center peak in the F_1 projection may be attributed to an artifact arising from the magnetizations which do not evolve in the t_1 period because of imperfection of the rf pulses. In the full 2D powder pattern, the above extra peaks emerge as the readily distinguished ridges almost parallel to the F_2 axis. As demonstrated in the previous section, only consideration of the residual chemical shifts in the t_1 period can give rise to such extra peaks or ridges; no matter how various spin parameters are adjusted, the F_1 projection would show a simple Pake pattern if we neglected the strong coupling or AB effects using the A_2 approximation (Figure 6b). In fact, the observed spectrum can satisfactorily be reproduced by the exact calculation (Figure 6c), for which we assumed the noncollinear orientations for the two ^{31}P chemical shift tensors, as we will explain in detail below.

The information on the ^{31}P–^{31}P pairs in tetraphenyldiphosphine obtained from the spectral simulations is as follows. First, the effective coupling constant was determined to be $D_{eff} = \pm 3330$ Hz with an error of ± 100 Hz. If we ignored the J contribution, the P–P distance would be evaluated to be 2.280 ± 0.02 Å, being rather long and so necessitating consideration of the anisotropic J coupling,[10] which is expected for such directly bonded spin pairs consisting of heavy atoms ^{31}P. From the magnitude $|D_{eff}|$, the value of the J anisotropy is evaluated to be $\Delta J = +6960 \pm 100$ or $+300 \pm 100$ Hz by assuming a typical P–P distance of 2.215 Å[19] or a dipolar coupling constant $D = -3630$ Hz. One of the important points when taking into account the residual chemical shift effects is that the spectral analysis may yield the otherwise unobtainable isotropic J coupling for homonuclear coupled spin pairs. The spectral simulations yield the value of $J_{iso} = \pm 200 \pm 100$ Hz. The positive and the negative values of J_{iso} respectively correspond to the effective couplings D_{eff} of $+3330$ and -3330 Hz or the ΔJ values of $+6960$ and $+300$ Hz; the powder patterns calculated by assuming these combinations of the relative signs of J_{iso} and D_{eff} can be distinguished from those calculated with the other combinations, as previously demonstrated in Figure 5. Furthermore, given that the magnitudes of the isotropic value and the anisotropy of the J coupling are expected to be of the same order,[3c,10c,d] the ambiguity in the absolute signs of J_{iso} and D_{eff} and that in the value of ΔJ are removed; namely, $J_{iso} = -200$, $D_{eff} = -3330$, and $\Delta J = +300$ Hz. It may be worth emphasizing that the ambiguity was eliminated after obtaining the magnitude of J_{iso} by considering the residual chemical shift effects. The determined magnitude and sign of the isotropic J coupling of tetraphenyldiphosphine is comparable with the reported values for other diphosphines in solutions.[20]

From the simulations of the 2D powder pattern, it was deduced that the chemical shift (shielding) components of the two ^{31}P were identical, namely, $\sigma_{11} = \sigma_{22} = -17$ and $\sigma_{33} = -57 \pm 5$ ppm (from H_3PO_4 85% aqueous solution) for both the nuclei, while the MAS spectrum exhibits a main peak at -30.7 ± 0.3 ppm, indicating a single average value of the shift components. This may be reasonable because the two phosphorus atoms are considered to be situated in similar environments in the molecule. On the other hand, it is surprising that the chemical shift tensors are axially symmetric around the σ_{33} (most shielded) axis in spite of the absence of such geometrical symmetry; note that, because of the dipolar coupling, the F_2 projections of the 2D spectra (Figure 6) are very different from the powder patterns arising only from such axially symmetric chemical shifts. For similar compounds tetraethyldiphosphine disulfide and tetrabuthyldiphosphine disulfide, however, a single-crystal NMR study revealed that the ^{31}P chemical shift tensor is also close to axially symmetric around the σ_{33} direction, and, more importantly, this most shielded axis was found to lie almost along the P=S direction,[10a] which falls on one of the apexes of the phosphorus pyramidal environment and the direction of the highest electron density around the phosphorus atom. It is therefore plausible that the ^{31}P nuclei in tetraphenyldiphosphine of the present interest may possess such symmetric chemical shift tensors whose unique $\sigma_{\parallel}$ ($=\sigma_{33}$) axes may be directed toward the lone pair electrons (Figure 7).

(18) Nakai, T.; McDowell, C. A. *Chem. Phys. Lett.* **1994**, *217*, 234–238.

(19) Richter, R.; Kaiser, J.; Sieler, J.; Hartung, H.; Peter, C. *Acta Crystallogr.* **1977**, *B33*, 1887–1892.

(20) (a) Lynden-Bell, R. M. *Trans. Faraday Soc.* **1961**, *57*, 888–892. (b) Aime, S.; Harris, R. K.; McVicker, E. M.; Fild, M. *J. Chem. Soc., Chem. Commun.* **1974**, 426–427; (c) *J. Chem. Soc., Dalton Trans.* **1976**, 2144–2153. (d) Christina, H.; McFarlane, E.; McFarlane, W. *J. Chem. Soc., Chem. Commun.* **1975**, 582–583.

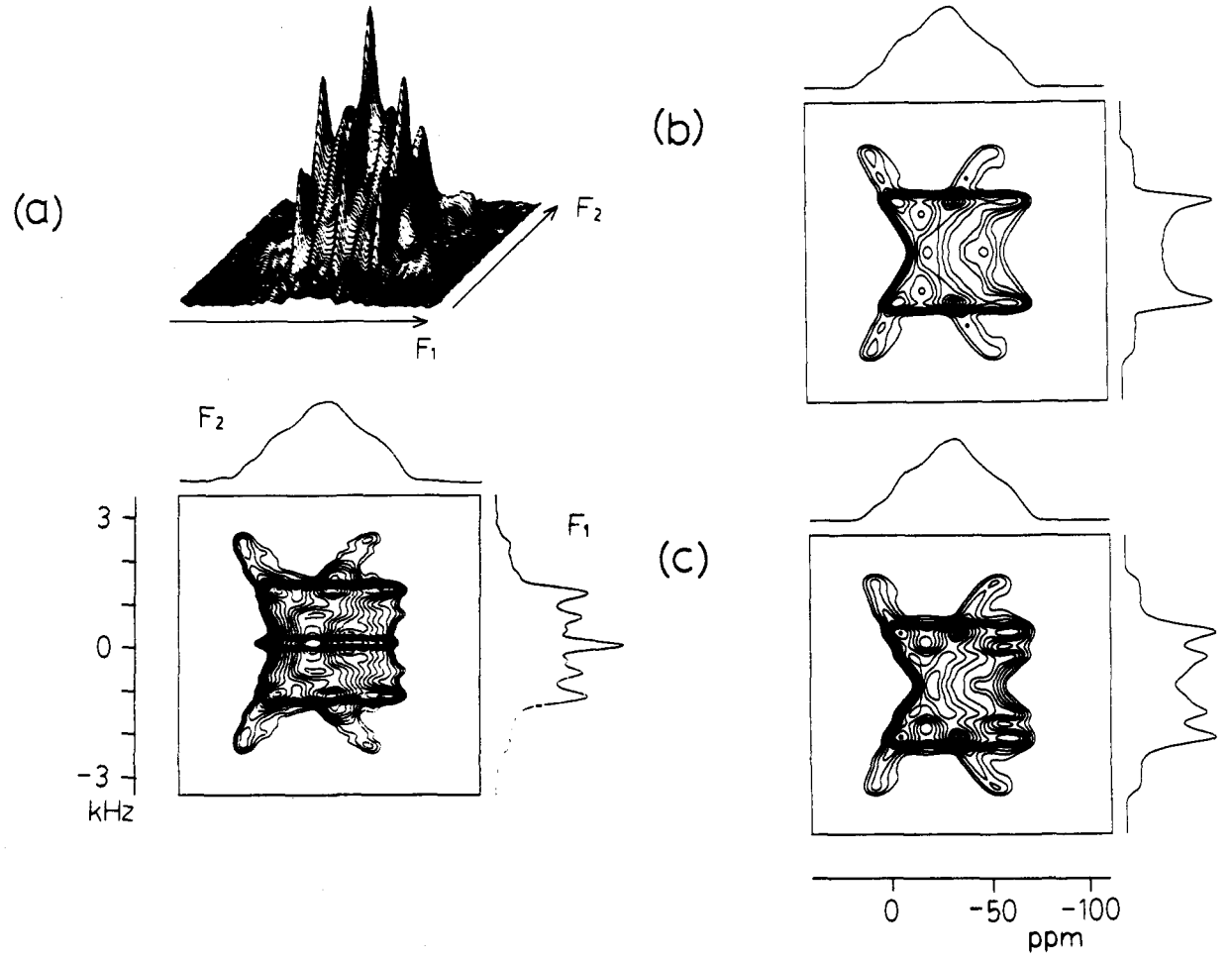

Figure 6. ^{31}P 2D spin-echo powder patterns for tetraphenyldiphosphine. (a) Experimental. Calculated (b) in the A_2 approximation and (c) without approximations. The spin parameters used for the calculations are given in the text.

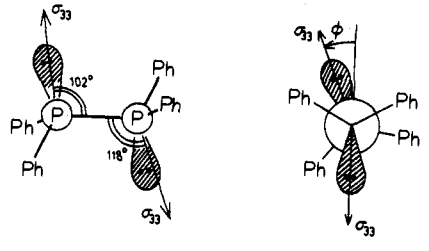

Figure 7. Molecular structure of tetraphenyldiphosphine. The σ_{33} axes of the ^{31}P chemical shift tensors toward the lone pairs of electrons are depicted.

Since the ^{31}P chemical shift tensors in tetraphenyldiphosphine were found to be axially symmetric around their σ_{33} axes, the relative orientations of these tensors and the P–P internuclear direction are specified by three angles: two angles between the P–P direction and the σ_{33} axes of the two individual chemical shift tensors and one torsion angle of the σ_{33} axes around the P–P direction. The former angles are evaluated to be 102 ± 10° and 118 ± 10°, close to the tetrahedral angle, and this fact strongly supports the view that the most shielded axes lie along the directions of the highest electron density or the lone pairs of electrons of the phosphorus atoms. If this is the case, the torsion angle of the σ_{33} axes corresponds to the dihedral angle of the lone pairs of electrons and the phosphorus atoms or the deviation angle from the *trans* conformation of the molecule (Figure 7). This angle ϕ is found to be as small as 18 ± 5°, indicating nearly *trans* geometry. The conformation was determined with high certainty since the 2D powder patterns are very sensitive to the torsion angle ϕ, as demonstrated in Figure 8; clearly, other conformations such as the *cis*-eclipsed (ϕ = 180°) and the *gauche* (ϕ = 120°) forms are eliminated, and furthermore, the slight distortion of 18° from the *trans* form is assured by referring to the spectra calculated for ϕ = 10° and 30°. The experimental F_1 projection might be similar to that calculated assuming the angle ϕ between 150° and 180°, but the observed 2D ridge, especially around F_2 = 0 ppm, does not agree with such a calculation. The present result concerning the molecular geometry seems to contradict theoretical and experimental studies for similar systems R_2XXR_2; MO (molecular orbital) calculations revealed that the most stable conformation for this type of molecules is *gauche*,[21] and liquid-state NMR studies indeed supported this conformation for some diphosphines.[20b,d] However, it is not unusual that the conformation in crystalline systems is different from that predicted or determined for isolated molecules,[21] and in fact X-ray studies clarified the eclipsed form (ϕ = 67°) for tetracyclohexyldiphosphine (R = C_6H_{10}, X = P)[19] and the *trans* form (ϕ = 0°) for tetraphenyldibismuth (R = C_6H_5, X = Bi),[22] for example. This may be rationalized by the fact that the conformation of a molecule in solids is greatly affected by the intermolecular packing forces and the intramolecular steric forces between the bulky residues R having fixed orientations in crystalline systems. Therefore, we believe that the present solid-state NMR study yields the correct geometry of the slightly distorted *trans* conformation for tetraphenyldiphosphine in the crystalline system.

Sodium Pyrophosphate Decahydrate. Polyphosphate anions, comprised of pyramidal PO_4 groups bonded through bridging oxygens O_B, are important systems in phosphorus chemistry, and

(21) Cowley, A. H.; White, W. D.; Damasco, M. C. *J. Am. Chem. Soc.* **1969**, *91*, 1922–1928.
(22) Carderazzo, F.; Poli, R.; Pelizzi, G. *J. Chem. Soc., Dalton Trans.* **1984**, *2365*–2369.

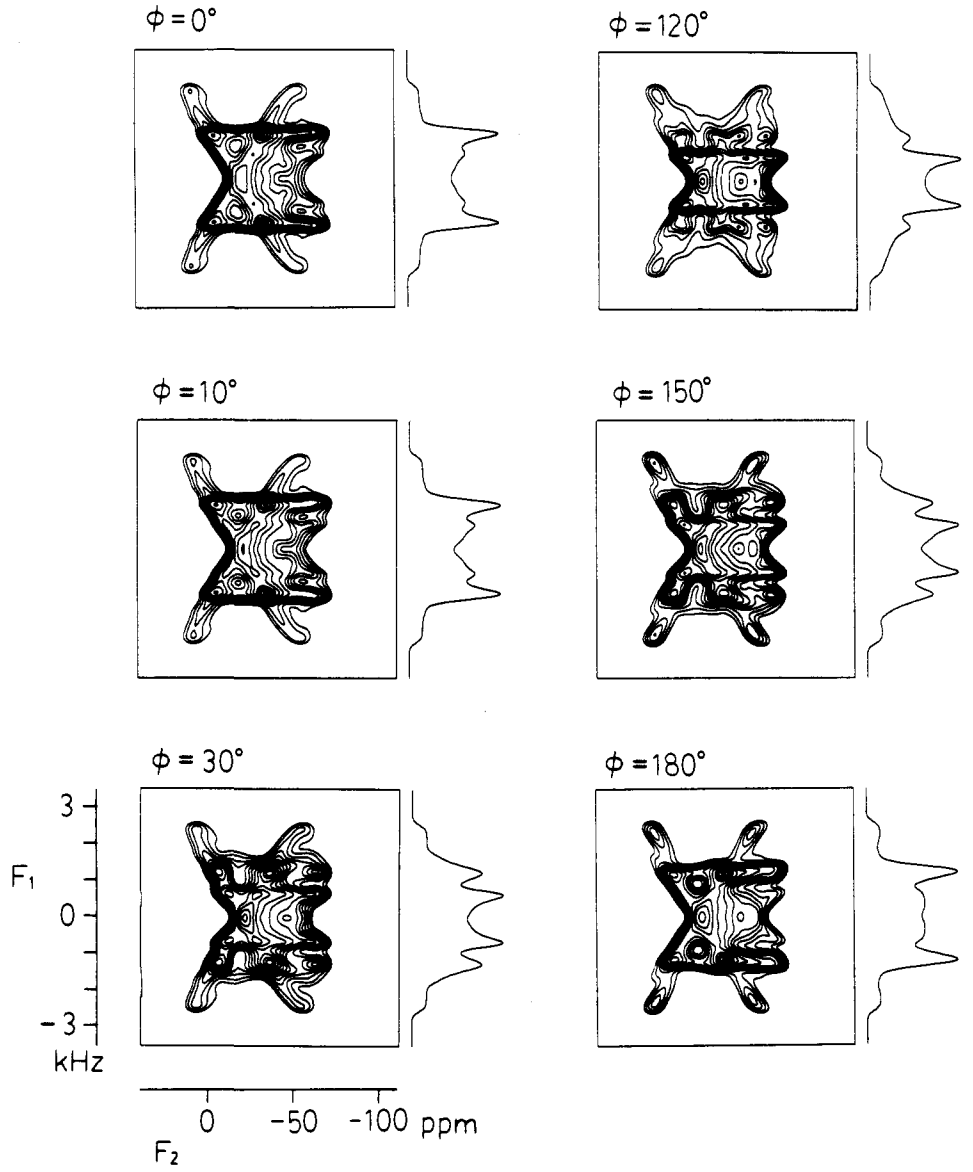

Figure 8. ^{31}P 2D spin-echo powder patterns for tetraphenyldiphosphine calculated with various values of the angle ϕ, which is defined in Figure 7 and signifies the conformation of the molecule.

the interesting electronic structures around the phosphorus atoms have often been discussed in terms of ^{31}P chemical shifts.[23] However, most of the solid-state NMR studies for polyphosphates have examined powdered samples by conventional techniques, giving no information about the orientations of the interaction tensors.[23c-h] In the present study on the 2D spin-echo powder patterns, we attempt to provide this information using a polycrystalline sample of sodium pyrophosphate decahydrate, where the anion is comprised of two PO_4 groups and is a classical example of ^{31}P spin pair systems.

Figure 9a shows the ^{31}P 2D spin-echo powder pattern observed for sodium pyrophosphate decahydrate. The F_2 projection or the conventional 1D dipolar/chemical shift powder pattern is similar to a single axially symmetric powder pattern for chemical shifts only, and the subtle additional singularities indicated by arrows in the spectrum are almost smeared out by the broadening. Hence, one may be tempted to neglect the dipolar coupling for the non-directly-bonded spin pair $^{31}P-O_B-^{31}P$, which is in fact as small as 1–2 kHz, in comparison with the chemical shift anisotropy. It is this low resolution of the conventional 1D powder patterns[23c,d,f,g] that has prevented such works from yielding the tensor orientations, which can be determined only when the dipolar couplings are observed in addition to the chemical shifts. On the other hand, however, the singularities become evident in the full 2D powder pattern, as shown in Figure 9a, because of the comparatively high spectral resolution, exhibiting the notable 2D ridges which enable us to determine the spin parameters accurately.

In simulating the experimental 2D powder pattern for sodium pyrophosphate decahydrate, we first examine whether the chemical shifts are not perfectly refocused to show some influences on the spectra along the F_1 axis; if the dipolar coupling is sufficiently small, it can be assumed not to interfere with the refocusing of the chemical shifts. In other words, we examine the spectra for the $^{31}P-^{31}P$ spin system in this compound to see if it can be described using the A_2 approximation; the two phosphorus nuclei are related to each other by the C_2 symmetry operation,[24] and so the equivalent environments around these

(23) (a) Kohler, S. J.; Ellet, J. D., Jr.; Klein, M. P. *J. Chem. Phys.* **1976**, *64*, 4451–4458. (b) Herzfeld, J.; Griffin, R. G.; Haberkorn, R. A. *Biochemistry* **1978**, *17*, 2711–2718. (c) Grimmer, A.-R. *Spectrochim. Acta* **1978**, *34A*, 941–941. (d) Duncan, T. M.; Douglass, D. C. *Chem. Phys.* **1984**, *87*, 339–349. (e) Turner, G. L.; Smith, K. A.; Kirkpatric, R. J.; Oldfield, E. *J. Magn. Reson.* **1986**, *70*, 408–415. (f) Burlinson, N. E.; Dunnell, B. A.; Ripmeester, J. A. *J. Magn. Reson.* **1986**, *67*, 217–230. (g) Un, S.; Klein, M. P. *J. Am. Chem. Soc.* **1989**, *111*, 5119–5124. (h) Hayashi, S.; Hayamizu, K. *Bull. Chem. Soc. Jpn.* **1989**, *62*, 3061–3068. (i) Kubo, A.; McDowell, C. A. *J. Chem. Phys.* **1990**, *92*, 7156–7170.

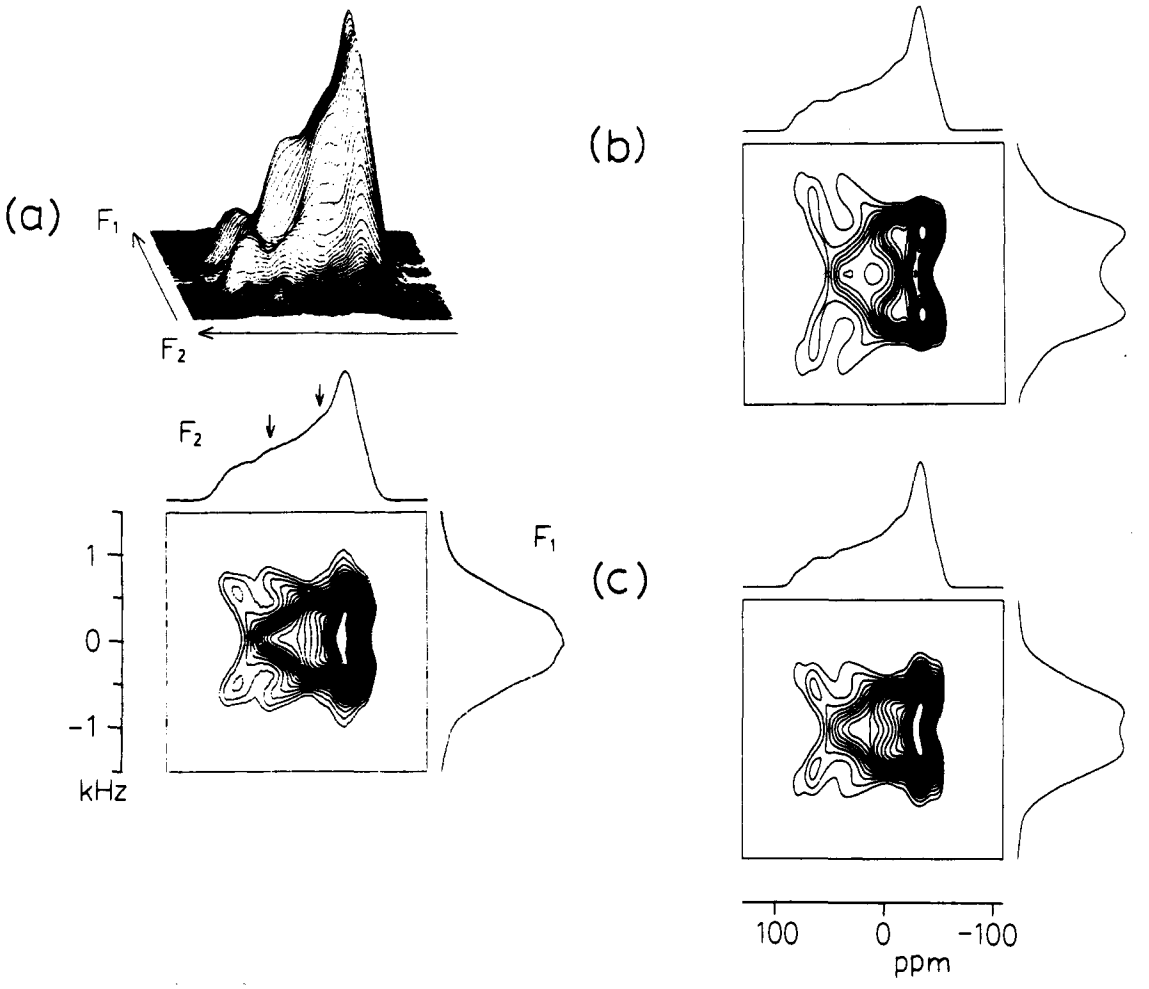

Figure 9. ^{31}P 2D spin-echo powder patterns for sodium pyrophosphate decahydrate. (a) Experimental. Calculated (b) in the A_2 approximation and (c) without approximations. The spin parameters used for the calculations are given in the text.

nuclei may render at least their chemical shift components identical. In Figure 9b is demonstrated the calculated spectrum for this compound based on the A_2 approximation, where we assumed the value of dipolar coupling constant of $D = -1580$ Hz ($r_{PP} = 2.925$ Å[24]); we neglected the isotropic and the anisotropic J couplings between these non-directly-bonded spins, for which typically $|^2J_{iso}(P\text{–}O\text{–}P)| = 20$ Hz,[25] and considered only the much larger dipolar coupling. The width of the A_2-approximated F_1 line shape is very different from that of the experimental spectrum, to which the residual chemical shifts indeed contribute; if we reproduce the experimental line width using the A_2 approximation, we would have to assume an unreasonably long internuclear distance of 3.35 Å. On the other hand, the exact calculation assuming the same dipolar coupling constant (Figure 9c) yields the spectral width along the F_1 axis in a good agreement with the experimental one, and the internuclear distance of $r_{PP} = 2.925$ Å[24] was confirmed with an error of ±0.04 Å. Thus, we can emphasize the necessity of including the residual chemical shift effects in the F_1 dimension for this compound.

The chemical shift (shielding) components for sodium pyrophosphate decahydrate obtained by simulating the 2D powder pattern are $\sigma_{11} = 76$, $\sigma_{22} = -34$, and $\sigma_{33} = -48 \pm 5$ ppm. The values of the shift components are significantly different from those[23h] obtained from what is called Herzfeld and Berger's analysis[26] for the MAS sideband intensities but are similar to those determined both in a novel sideband analysis considering the dipolar coupling and in a single-crystal measurement.[23i] As

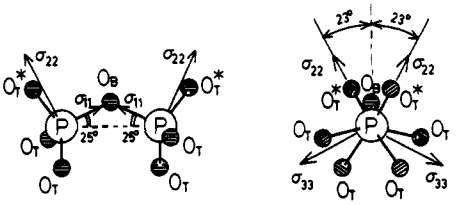

Figure 10. Structure of the pyrophosphate anion in sodium pyrophosphate decahydrate. The principal axes of the ^{31}P chemical shift tensors proposed in the present study are also depicted.

is well known, Herzfeld and Berger's method is valid only for isolated spins, such as natural abundance ^{13}C systems, and cannot reproduce the effects of homonuclear dipolar couplings on the spinning sidebands.[16c,d,23i] It follows that, using this method, not only the tensor orientations cannot be obtained but also the estimated shift components involve systematic errors, although many MAS sideband studies for polyphosphates have improperly employed the method.[23d,f–h] In contrast, for the present static powder patterns, the theoretical treatment for the homonuclear coupling is straightforward and exact, yielding correct chemical shift components.

It should be noted that the chemical shift tensor is close to axially symmetric around the σ_{11} (least shielded) axis. Furthermore, the spectral simulation clarified that the σ_{11} axis for each ^{31}P nucleus makes an angle of 25 ± 5° with the P–P internuclear vector and all these three axes are coplanar, while the P–O_B–P angle is reported to be 130°.[24] Therefore, we can interpret the σ_{11} axes of both of the ^{31}P nuclei to coincide with the individual P–O_B bond directions (Figure 10, left), in spite of

(24) McDonald, W. S.; Cruickshank, D. W. J. *Acta Crystallogr.* **1967**, *22*, 43–48.
(25) Gorenstein, D. G. *Phosphorus-31 NMR*; Academic: New York, 1984.
(26) Herzfeld, J.; Berger, A. E. *J. Chem. Phys.* **1980**, *73*, 6021–6030.

the ambiguity arising from the overall rotation around the P–P axis. The chemical shift direction may conspicuously reflect such electronic structures of the end PO_4 groups in polyphosphate anions that, because of the single-bond character of the P–O_B bond, the multiple- or π-bond character is transferred to the other three bonds between the phosphorus and the terminal oxygens O_T.[27] The electron density may thus be axially symmetric around the P–O_B bond and comparatively low in this bond direction, being consistent with the least shielded (σ_{11}) direction determined here. While the above conclusion was first drawn in a single-crystal NMR study for α-calcium pyrophosphate,[23a] the present work confirms it, using a polycrystalline sample, with a novel measurement of the 2D spin-echo powder pattern.

On the other hand, the small nonaxial symmetry of the ^{31}P chemical shift tensors in pyrophosphates[23a,d,g,i] has not been well interpreted. In a semiempirical way, Burlinson *et al.* explained the asymmetry found for the end ^{31}P nuclei in a triphosphate anion;[23f] the part of the anion other than the end PO_4 group of interest, whose geometry is, of course, different from the axial symmetric around the P–O_B bond, may affect the anisotropic chemical shifts directly or indirectly by modifying the geometry of the PO_4 group. The σ_{22} direction for sodium pyrophosphate decahydrate is found to be similar to that deduced for the triphosphate;[23f] the σ_{22} axis is almost on the P–O_B–P plane, with a slight deviation in the direction rotated around the P–O_B(σ_{11}) axis by 20 ± 10° away from the plane. Furthermore, the small deviation of the σ_{22} axis from the P–O_B–P plane may be attributable to the configuration of the terminal oxygens O_T. The $P_2O_7^{4-}$ anion in sodium pyrophosphate decahydrate has a staggered form,[24,28] where one of the terminal oxygen atoms attached to one phosphorus atom, depicted as O_T* in Figure 10, is located as rotated by 23° about P–O_B away from the P–O_B–P plane in the opposite direction of that for O_T* attached to the other phosphorus atom (Figure 10, right), so that the intramolecular steric forces between the terminal oxygens may be decreased. For the particular terminal oxygen atoms O_T* slightly out of the plane, the O_T*–P–O_B angle (102°) is significantly smaller than the other two O_T–P–O_B angles (109° and 107°).[24] Therefore, it is plausible that this oxygen may cause the electronic environment around the phosphorus atom to have a special direction along the corresponding P–O_T* bond, rendering one of the ^{31}P shift tensor axes (σ_{22} axis) coplanar with the O_T*–P–O_B plane. Thus, in addition to the reported empirical rule that the magnitudes of the ^{31}P chemical shift anisotropies are proportional to the variations of the O–P–O angles,[23e,g] we here obtained novel information on the principal axis directions of the chemical shift tensors related to the O_T–P–O_B angles, although these effects have not been well explained theoretically.

1,2-^{13}C Doubly-Labeled Palmitic Acid. In contrast to the spin systems discussed in the previous sections, we here treat a spin pair having a large difference of the (isotropic) chemical shifts of involved magnetic nuclei, namely, palmitic acid labeled with ^{13}C at the sites of the carboxylic carbon C_1 and the neighboring α-methylene carbon C_2. The spin parameters obtained from spectral simulations using such labeled molecules may yield some important information on this compound; for example, similar to other fatty acids,[29] a variety of polymorphism known for palmitic acid[29a-c] may probably be related to the geometry of the carboxylic end group.[29g] In the present study, we attempt to obtain the characteristic features of *C*-form palmitic acid, which is, among various polymorphic forms, the one most easily recrystallized and stable at room temperature.

Figure 11a shows the ^{13}C 2D spin-echo powder pattern observed for 1,2-^{13}C doubly-labeled palmitic acid. The F_1 projection of the 2D spectrum exhibits a distinct Pake pattern, apart from the artifact peak around the center ($F_1 = 0$). The separation of the singularities in this Pake pattern, 2.2 kHz, leads to a reasonable C_1–C_2 bond distance of $r_{CC} = 1.50 \pm 0.03$ Å if equated to the theoretical expression in the AX approximation $\gamma^2\hbar/r_{CC}^3$; the isotropic *J* coupling of about 60 Hz[16c,d] and the *J* anisotropy of the same order are so small compared with the dipolar coupling that they may be neglected in the stationary powder patterns. Therefore, one may suppose that the spin pair of the present interest can be described as an AX system, similar to heteronuclear spin systems. In fact, the 2D powder pattern calculated on the basis of the AX approximation (Figure 11b) can reproduce the experimental one very well, and also it is almost entirely identical with the spectrum calculated in the exact manner (Figure 11c), except for the small ridges indicated by arrows in the figure. Whether this slight difference is important or not should be judged in terms of the deduced spin parameters, which we will discuss below, and here we can assume that the AX calculation yields a good approximated spectrum for the present spin system.

The principal components of the ^{13}C chemical shift (shielding) tensors (σ_{11}, σ_{22}, σ_{33}) obtained from the simulations of the experimental 2D powder pattern are (237, 200, 109) ppm for the carboxylic carbon and (58, 39, 8) ppm for the α-methylene carbon (relative to tetramethylsilane), with a typical error of ±5 ppm. Furthermore, the presence of the dipolar coupling between the two carbons allows the deduction of the following information on the relative principal axis orientations of the interaction tensors. First, in the chemical shift principal axis system for the carboxylic carbon C_1, the polar and the azimuthal angles specifying the C_1–C_2 vector direction were found to be (β_1, α_1) = (90°, 42°). Namely, the σ_{33} axis is perpendicular to the C_1–C_2 vector. Hence, we can regard this axis as to be normal to the COO plane (Figure 12), as is usually the case with sp^2-hybridized carbons,[30] even though the angle between the σ_{33} axis and the COO plane cannot be determined in a unique way because of the ambiguity mentioned earlier. With regard to the σ_{11} axis, while it is known to be parallel to the C_1–C_2 direction for the systems having two equivalent CO bonds,[30] the large deviation of 42 ± 10° obtained for *C*-form palmitic acid suggests that the two CO bonds are inequivalent: one is a single bond (C—OH) and the other a double bond (C=O). In other words, exchange motions of protons along the hydrogen bonds in a dimer comprised of two palmitic acid molecules may be frozen in the time scale of NMR spectroscopy. This result is consistent with the geometry reported for a similar system of the *C*-form of stearic acid, where the bond distances are 1.39 Å for C—OH and 1.24 Å for C=O,[29g] while in the *B*-form of the same compound, the two CO bonds are almost equivalent, 1.30 and 1.28 Å.[29h] Thus, we can conclude that the present NMR study clarified one of the characteristic features of *C*-form palmitic acid which may differ from that of the *B*-form counterpart, although no detailed X-ray studies for this compound have been reported.

On the other hand, the C_1–C_2 vector direction in the chemical shift principal axis system of the methylene carbon C_2 was found to be specified by the angles (β_2, α_2) = (47°, −90°). The σ_{11} axis is thus perpendicular to the C_1–C_2 vector, and so we can consider, for the reason similar to that discussed above for the carboxylic carbon, that this axis is normal to the plane containing the *trans*-methylene carbon chain (Figure 12); for the internal methylene

(27) Cruickshank, D. W. J. *J. Chem. Soc.* **1961**, 5486–5504.
(28) Calvo, C. *Inorg. Chem.* **1968**, *7*, 1345–1351.
(29) (a) Stenhagen, E.; von Sydow, E. *Ark. Kemi* **1953**, *6*, 309–319. (b) Verma, A. R. *Proc. R. Soc. London* **1955**, *A228*, 34–50. (c) von Sydow, E. *Acta Chem. Scand.* **1955**, *9*, 1685–1688; (d) *Ark. Kemi* **1956**, *9*, 231–254. (e) Holland, R. F.; Nielsen, J. E. *J. Mol. Spectrosc.* **1962**, *9*, 436–460. (f) Larsson, K.; von Sydow, E. *Acta Chem. Scand.* **1966**, *20*, 1203–1207. (g) Malta, V.; Celotti, G.; Zannetti, R.; Martelli, A. F. *J. Chem. Soc. B* **1971**, 548–553. (h) Goto, M.; Asada, E. *Bull. Chem. Soc. Jpn.* **1978**, *51*, 2456–2459.
(30) (a) Kempf, J.; Spiess, H. W.; Haeberlen, U.; Zimmermann, H. *Chem. Phys.* **1974**, *4*, 269–276. (b) Ackerman, J. L.; Tegenfeldt, J.; Waugh, J. S. *J. Am. Chem. Soc.* **1974**, *96*, 6843–6845. (c) Pines, A.; Chang, J. J.; Griffin, R. G. *J. Chem. Phys.* **1974**, *61*, 1021–1030. (d) Griffin, R. G.; Pines, A.; Pausak, S.; Waugh, J. S. *J. Chem. Phys.* **1975**, *63*, 1267–1271. (e) Griffin, R. G.; Ruben, D. J. *J. Chem. Phys.* **1975**, *63*, 1272–1275.

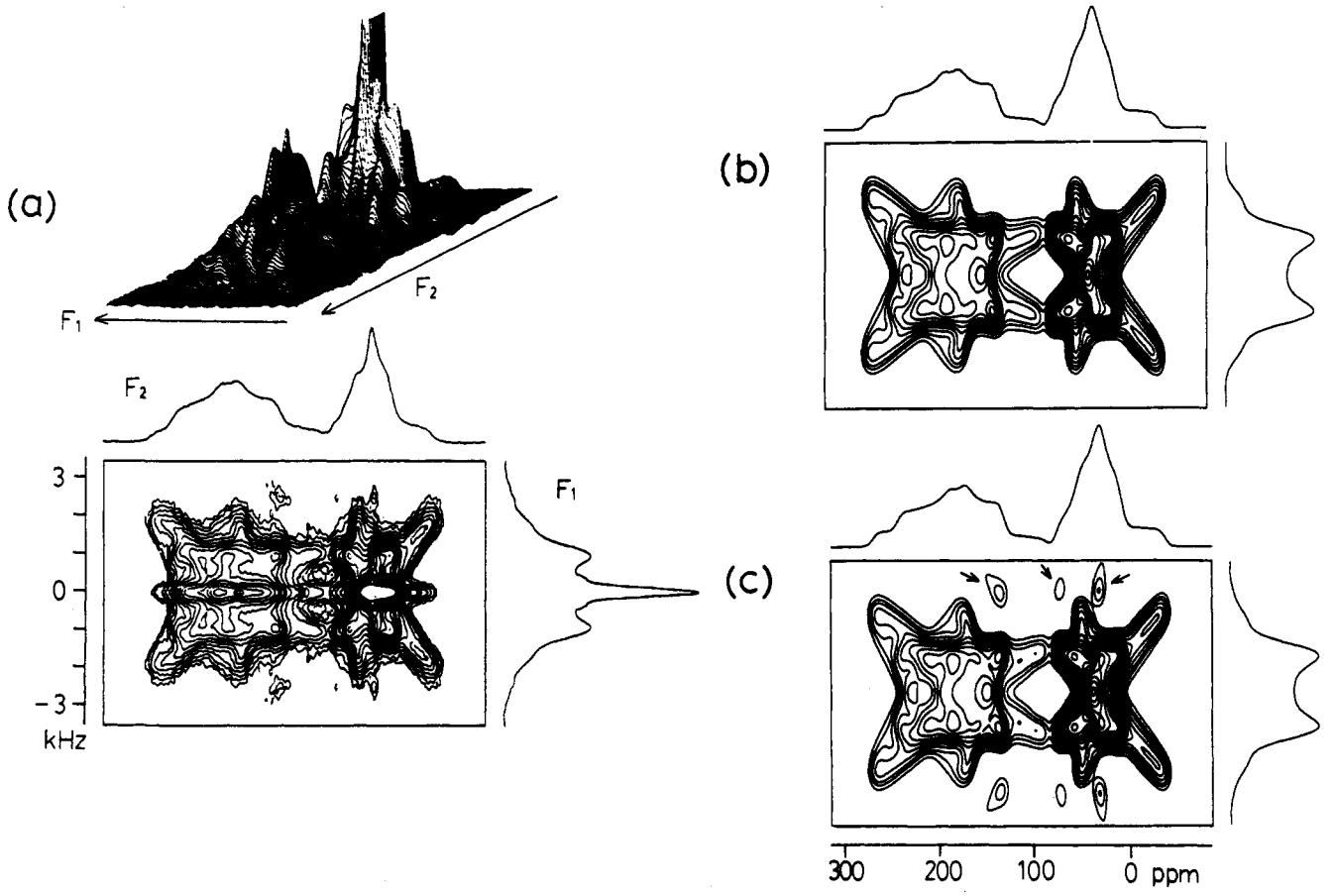

Figure 11. ^{13}C 2D spin-echo powder patterns for 1,2-^{13}C doubly-labeled palmitic acid. (a) Experimental. Calculated (b) in the AX approximation and (c) without approximations. The spin parameters used for the calculations are given in the text.

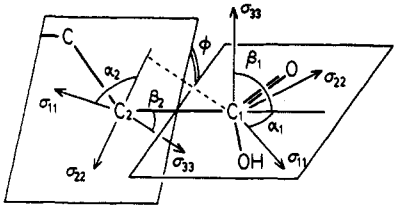

Figure 12. Principal axes of the ^{13}C chemical shift tensors for the carboxylic carbon C_1 and the α-methylene carbon C_2 in *C*-form palmitic acid.

carbons in a sufficiently long *trans* chain, it is reported that the σ_{11} axis is perpendicular to the chain plane and the σ_{33} axis parallel to the long axis direction of the chain.[31] The σ_{33} direction in this "ideal" system might lead to the polar angle of the C_1–C_2 vector, β_2 = 33.5°, by assuming the C–C–C angle of 113°, which is different from the value of 47 ± 5° determined for the α-methylene carbon in palmitic acid. This difference may be attributed to some crystalline field effects arising from the carboxylic group on the α-methylene carbon, which is located at the end of the chain, unlike the internal methylene carbons.

It may be of interest to determine the configuration of the carboxylic end group of fatty acids, namely, the relative orientation of the COO plane with respect to the plane involving the *trans*-methylene carbon chain. The orientations of these planes may be characterized by the chemical shift tensor axes, such as the σ_{33} axis of the carboxylic carbon and the σ_{11} axis of α-methylene carbon. It should be noted that the dihedral angle of these two planes ϕ is independent of β_i and α_i (i = 1, 2) specifying the C_1–C_2 dipolar axis direction in the individual C_i chemical shift tensor frames (Figure 12) but, instead, may represent the direct relation of the two chemical shift tensor orientations. We found that the angle ϕ is hardly reflected in the spectra calculated in the AX approximation, where the two spins are treated as heteronuclear-like spins. This may be well understood by recalling the fact that, for heteronuclear coupled spin systems, one spin species is not affected by the chemical shift Hamiltonian for the other species,[4a] and thereby the spectrum may reflect the correlation of the two chemical shift tensors only through the dipolar tensor. In contrast, the spectra calculated without such an approximation or with consideration of the AB effects may conspicuously reflect the dihedral angle ϕ; in Figure 13 are shown the 2D powder patterns thus calculated by assuming various values of ϕ. Clearly, the positions of the small ridges, which do not appear in the AX-approximated spectra (Figure 11b), are sensitive to this parameter. From the values reproducing the positions of the relevant ridges in the experimental spectrum (Figure 11a), we estimate the dihedral angle ϕ = 10 ± 10°. Thus, it is demonstrated that, even for the present spin pair having a large chemical shift difference, the exact calculations are necessary to obtain this important parameter, in contrast to the reported study assuming the AX approximation.[5c] The dihedral angle evaluated for *C*-form palmitic acid is in good agreement with ϕ = 10.3° in *C*-form stearic acid,[29s] markedly differing from ϕ = 75.4° in the *B*-form of the same compound.[29f] Thus, the present study for palmitic acid has revealed another aspect specific to the *C*-form crystalline systems.

Conclusions

In the present paper, we have described both the theoretical and the experimental details of special 2D spectra for homonuclear coupled spin pair systems in static polycrystalline samples; the 2D rf pulse sequence, where the spin-echo subsequence is incorporated in the evolution (t_1) period, exhibits conspicuous signal distributions in the 2D frequency plane, namely, 2D spin-

(31) VanderHart, D. L. *J. Chem. Phys.* **1976**, *64*, 830–834.

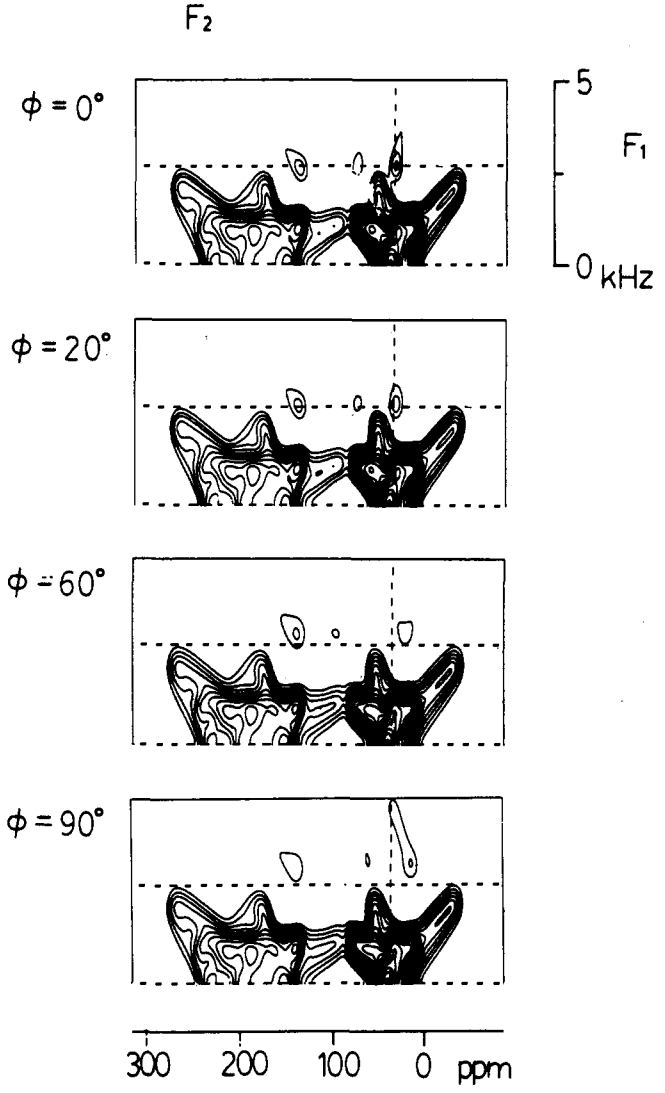

Figure 13. ^{13}C 2D spin-echo powder patterns for 1,2-^{13}C doubly-labeled palmitic acid calculated with various values of the dihedral angle ϕ of the COO plane and the methylene chain plane, which is defined as shown in Figure 12.

echo powder patterns. The 2D spectra can yield not only the principal components of the interaction tensors but also their relative principal axis orientations with high accuracy, which have usually been obtained only in single-crystal NMR studies. The comparatively high resolution of the 2D powder patterns allows us to determine the parameters accurately, whereas the conventional 1D powder patterns are often not sensitive to the spin parameters.

Much theoretical attention has been paid to the effects of the spin-echo sequence to homonuclear spin pairs; the theory is straightforward but would be tedious without the product operator formalism which we recently developed to be applicable to strongly coupled spin systems[14] and employed in the present study. We demonstrated by the exact calculations that, in general, the sequence cannot perfectly refocus the evolution arising from chemical shifts in the t_1 period, but the chemical shift anisotropies may contribute to the spectra in the corresponding frequency (F_1) dimension. These residual chemical shift effects have been verified in the analysis of the experimental 2D spin-echo powder patterns, for which the AX or the A_2 approximation has been employed by assuming the complete refocusing of the chemical shifts.[5] The exact calculations which we presented in this study are generally necessary to analyze the experimental spectra, since the validity of the AX and the A_2 approximations, which is subject to various spin parameters unknown before the analysis, is not guaranteed.

The fact that the dipolar (and J) couplings are not completely separated from the chemical shifts may not be a disadvantage of the method of the 2D spin-echo powder patterns. Not only are there no difficulties in the spectral analysis because we explicitly formulated the resonance frequencies and intensities reflecting the residual chemical shift effects, but also these effects may yield information otherwise unobtainable when they are neglected; we can evaluate the isotropic J couplings for the spin pairs having identical chemical shift components, which cannot be taken into account in the A_2 approximation, and also we can obtain the direct relation of the orientations of the two chemical shift tensors, which cannot be reflected in the AX-approximated spectra.

We applied the method of the 2D spin-echo powder patterns to three different spin pair systems and discussed the electronic environments of the magnetic nuclei and the geometry of the molecules. It was found that the ^{31}P chemical shift tensor in tetraphenyldiphosphine is axially symmetric around the most shielded (σ_{33}) axis, which lies along the lone pair of electrons of the phosphorus atom. Also, it was shown that the lone pairs and the phosphorus atoms form a nearly *trans* conformation in crystalline systems. For sodium pyrophosphate decahydrate, the ^{31}P chemical shift tensor is, on the other hand, almost axially symmetric around the least shielded (σ_{11}) axis, and this unique-axis direction was found to coincide with the P–O_B (bridging oxygen) direction. It was suggested that the slight nonaxial symmetry of the ^{31}P chemical shift tensor may reflect variation of the O_B–P–O_T (terminal oxygens) angles and the σ_{22} directions of the two ^{31}P nuclei may manifest the staggered form[24,28] of the pyrophosphate anion in this compound. For palmitic acid, we clarified, from the orientations of the ^{13}C chemical shift tensors, the geometry characteristic of the molecules in the *C*-form crystalline systems,[29g] namely, the inequivalence of the two CO bonds and the intrinsic dihedral angle of the COO plane and the methylene chain plane. A further study for *B*-form palmitic acid and the phase transition between the above two forms is under investigation.

Acknowledgment. We thank the Natural Sciences and Engineering Research Council (NSERC) of Canada for research grants to C.A.M. We also thank Dr. Robin Challoner, University of Durham, U.K., for the fruitful discussions on ^{31}P chemical shifts and for drawing our attention to key references.